Mathematics for input space probes in the atmosphere of Gliese 581d

R. Gobato[1], A. Gobato[2] and D. F. G. Fedrigo[3]

Abstract

The work is a mathematical approach to the entry of an aerospace vehicle, as a probe or capsule in the atmosphere of the planet Gliese 581d, using data collected from the results of atmospheric models of the planet. GJ581d was the first planet candidate of a few Earth masses reported in the circum-stellar habitable zone of another star. It is located in the Gliese 581 star system, is a star red dwarf about 20 light years away from Earth in the constellation Libra. Its estimated mass is about a third of that of the Sun. It has been suggested that the recently discovered exoplanet GJ581d might be able to support liquid water due to its relatively low mass and orbital distance. However, GJ581d receives 35% less stellar energy than the planet Mars and is probably locked in tidal resonance, with extremely low insolation at the poles and possibly a permanent night side. The climate that demonstrate GJ581d will have a stable atmosphere and surface liquid water for a wide range of plausible cases, making it the first confirmed super-Earth (2-10 Earth masses) in the habitable zone. According to the general principle of relativity, "All systems of reference are equivalent with respect to the formulation of the fundamental laws of physics." In this case all the equations studied apply to the exoplanet Gliese 581d. If humanity is able to send a probe to Gliese 581d, this has all the mathematical conditions set it down successfully on its surface.

Keywords

Aerodynamic, Astrobiology, Atmosphere, Exoplanet, Gliese 581d, GJ581d, Red dwarf, Space vehicle.

[1] *Laboratório de BioFísica e Dinâmica Molecular Computacional, CEJC, Rua Rocha Pombo, 953, Centro, Bela V. do Paraíso/PR, 86130-000, Brasil.*

[2] *Faculdade Pitágoras Londrina, Rua Edwy Taques de Araújo, 1100, Gleba Palhano, Londrina/PR, 86047-500, Brasil.*

[3] *Aeronautical Engineering Consulting, Consultant in processes LOA/PBN RNAV, Rua Luísa, 388s, Vila Portuguesa, Tangará da Serra/MT, 78300-000, Brasil.*

Corresponding authors: [1]ricardogobato@seed.pr.gov.br; [2]alekssandergobato@hotmail.com; [3]desirefg@bol.com.br

Introduction

Gliese 581d, Gl581d, GJ 581d

GJ 581d was the first planet candidate of a few Earth masses reported in the circum-stellar habitable zone of another star. It is located in the Gliese 581 star system, in the constellation Libra, a red dwarf (20.3 ly from the Sun, $M = 0.31 M_{Sun}$, $L = 0.0135 L_{Sun}$, spectral type M3V) [1, 2] has received intense interest over the last decade due to the low mass exoplanets discovered around it. Coordinate: right ascension $15^h 19^m 26.8250^s$, declination -07° 43' 20.209", apparent magnitude 10.56 to 10.58, distance 20.4 ± 0.2 ly (6.25 ± 0.05 pc). As of early 2011 it has been reported to host up to six planets. [3, 4, 5, 6] One of these, GJ581g, was announced in September 2010 and estimated to be in the habitable zone (the orbital range in which a planet's atmosphere can warm the surface sufficiently to allow surface liquid water). [7, 8]

However, its discovery has been strongly disputed by other researchers, including the team responsible for finding the other four planets in the system. [9, 10] For the moment, therefore, GJ581g remains unconfirmed. [11, 12]

Its mass is thought to be 6.98 Earths($\oplus$) and its radius is thought to be $2.2R_{\oplus}$. It is considered to be a super-Earth, has a solid surface allowing for any water present on its surface to form liquid oceans and even landmasses characteristic of Earth's surface, although with a much higher surface gravity. Its orbital period is thought to be 66.87 days long, with a semi-major axis of 0.21847 with an unconfirmed eccentricity. [6, 13, 14]

Radiative-convective studies [15, 16, 17] have suggested that a dense atmosphere could provide a significant greenhouse effect on GJ581d. However, the planet's tidal evolution poses a key problem for its habitability. [12]

As it is most likely either in a pseudo-synchronous state with a rotation period that is a function of the eccentricity, or in spin-orbit resonance like Mercury in our Solar System (Leconte et al. 2010; Heller et al. 2011), GJ581d should have extremely low insolation at its poles and possibly a permanent night side. Regions of low or zero insolation on a planet can act as cold traps where volatiles such as H_2O and CO_2 freeze out on the surface. [11, 12]

A few previous studies (Joshi et al. 1997; Joshi 2003) have examined atmospheric collapse in 3D with simplified radiative transfer, but only for Earth-like atmospheric pressures or lower (0.1 to 1.5 bar). For low values of stellar insolation and large planetary radii, even dense CO_2 atmospheres will be prone to collapse, which could rule out a stable water cycle altogether for a super-Earth like GJ581d. To conclusively evaluate whether GJ581d is in the habitable zone, therefore, three-dimensional simulations using accurate radiative transfer are necessary. [11, 12]

GJ581d, in contrast, which was first discovered in 2007 and has a minimum mass between 5.6 and 7.1 M_{Earth}, has now been robustly confirmed by radial velocity (RV) observations [3](Udry et al. 2007; Mayor et al. 2009; Vogt et al. 2010). Due to its greater distance from the host star, GJ581d was initially regarded as unlikely to have surface liquid water unless strong warming mechanisms due to e.g., CO_2 clouds (Forget and Pier-rehumbert 1997; Selsis et al. 2007) were present in its atmosphere. Recently, simple one-dimensional. [11, 12]

In 2007, radial velocity measurements were used to discover two new planets in the Gl581 system. [3] These planets have captured much attention both in the community and among the general public, as their minimum masses were measured to be below 10 $M_{\oplus}$, and they are close to the edges of their system's nominal "habitable zone", i.e., the loosely defined orbital region in which planets can sustain liquid water on their surfaces. The first planet, Gl581c, which is closer to its star and was the first discovered, was initially estimated to be potentially habitable based on its equilibrium temperature Teq = 320 K, using an Earth-like planetary albedo 0.29. In contrast, the second planet Gl581d has an equilibrium temper-
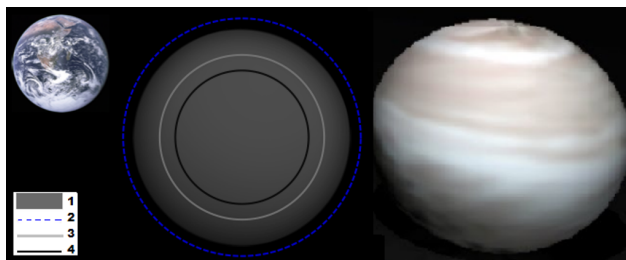

Figure 1. Comparison of several possible sizes for the exoplanet Gliese 581 d with the planet Earth and Gliese581d, using approximate models of planetary radius as a function of mass[20] for several possible compositions, based on mass reported in the UPR Arecibo. [6] Models include: 1. water world with a rocky core, composed of 75% H_2O, 3% Fe, 22% $MgSiO_3$; 2. hypothetical pure water (ice) planet, the largest size for Gliese 581 d without a significant H/He envelope; 3. rocky terrestrial "Earth-like" planet, composed of 67% Fe, 32.5% $MgSiO_3$; 4. hypothetical pure iron planet, Gliese 581 d's theoretical smallest size Gliese 581 d is not likely to be smaller than the iron planet, and will be considerably larger than the water planet if significant H or He is present. For non-transiting planets, all modeled sizes will be underestimates to the extent that the planet's actual mass is larger than the reported minimum mass. [21] (Adapted)

ature Teq = 195 K for an albedo of 0.2, which suggests it may be too cold to sustain surface liquid water. However, these analyses neglect any possible warming of the surface due to the planet's atmosphere. [11, 12]

GJ 581d was the first planet candidate of a few Earth masses reported in the circum-stellar habitable zone of another star. [4] It was detected by measuring the radial velocity variability of its host star using High Accuracy Radial Velocity Planet Searcher (HARPS). [4, 18] Doppler time series are usually modeled as the sum of Keplerian signals plus additional effects (e.g., correlations with activity). Detecting a planet candidate consists of quantifying the improvement of a merit statistic when one signal is added to the model. Approximate methods are often used to speed up the analyses, such as computing periodograms on residual data. Even when models are linear, correlations exist between parameters. Similarly, statistics based on residual analyses are biased quantities and cannot be used for model comparison. [19]

1. Atmospheric model

General model description

Von Paris et al. [16] computationally simulate one model for the atmosphere of Gliese 581d. A 1D, cloud-free radiative-convective column model was used for the calculation of the atmospheric structure, i.e. the temperature and pressure profiles for different Gl 581d scenarios.

The model is originally based on the one described by Kasting et al. (1984a) [22] and Kasting et al. (1984b) [23]. Further developments are described by e.g. Kasting (1988) [24], Kasting (1991) [25], Kasting et al. (1993) [7], Mischna

et al. (2000) [26] and Pavlov et al. (2000) [27]. Additional updates of the thermal radiation scheme of the model have been introduced by Segura et al. (2003). The model version used here is based on the version of von Paris et al. (2008) [28] where a more detailed model description is given. The current model uses the radiative transfer scheme MRAC in the IR (see the introduction of this scheme in von Paris et al. 2008) [28]. The water profile in the model is calculated based on the relative humidity distribution of Manabe and Wetherald (1967) [29]. Above the cold trap, the water profile is set to an isoprofile at the cold trap value.

The model considers N_2, H_2O, and CO_2 as atmospheric gases. Other radiative trace species might be present in the atmospheres of exoplanets (e.g. SO_2, O_3, or CH_4), which could alter the radiative budget significantly. But because the presence of these gases highly depends on the planetary scenario (e.g., outgassing, volcanism, formation, biosphere), our model atmospheres are restricted to the two most important greenhouse gases of the Earth's atmosphere (H_2O and CO_2), using N_2 as additional backgroundgas. This is based on the observation that in the solar system all terrestrial atmospheres (Venus, Earth, Mars, Titan) contain significant amounts of N_2.

Temperature profiles from the surface up to the midmesosphere are calculated by solving the equation of radiative transfer and performing convective adjustment, if necessary. The convective lapse rate is assumed to be adiabatic. Water profiles are calculated by assuming a fixed relative humidity profile (Manabe & Wetherald 1967) [29] through the troposphere.

CO_2 clouds

If CO_2 condensation occurs in the upper atmosphere of a planet, it should cause CO_2 cloud formation. This effect is observed for example in the present-day Martian mesosphere. [30] While there are still many unknowns associated with the microphysics of CO_2 clouds. The infrared scattering effect described by Forget & Pierrehumbert (1997) [31] is expected to be slightly less efficient when the star is M-class, because a greater portion of the incident stellar radiation is also scattered back to space. Nonetheless, the clouds still increase the surface warming by an amount that increases with Nc, up to a theoretical maximum of around 30 K at 40 bar for Nc = 105 kg^{-1}. [32]

Stellar spectrum

To better understand the differences in climate caused by the fact that Gliese 581 is an M-class star, we first performed simulations comparing G-class (Sol) and M-class (AD Leo) stellar spectra. In both cases we normalized the total fluxes to the same value F_m.

As can be seen, the clear pure CO_2 atmospheres under a G-class star collapse on the surface for pressures greater than about 3 bar, but when the star is M-class, temperatures continue to increase, reaching the water melting point at just over 10 bar and a maximum value at around 30 bar. The essential reason for this difference is that Rayleigh scattering, which has an optical depth $\tau_R \propto \lambda^{-4}$, has a much weaker effect on the red-shifted M-class stellar spectrum. [32]

Surface gravity

Sotin et al. (2007) [33] proposed a relationship between planetary mass and radius ($r/r_E = \alpha(M/M_E)\beta$, with α and β equal to 1.0 and 0.274 for rocky planets and 1.262 and 0.275 for ocean planets, respectively. Given this relation and the current uncertainties in Gl 581d's mass, we can expect the planet's surface gravity to be in the range 10-30 ms^{-2}. For a given atmospheric pressure, the CO_2 column amount ps/g (and therefore the total mass of the atmosphere) decreases with g. Hence the primary effect of increasing g, predictably, is to cool the surface.

Variations in g also change the adiabatic lapse rate, while leaving the CO_2 saturation pressure unaffected. Hence for a given CO_2 column amount the temperature profile varies with the gravity, which also influences the climate. These changes are important in determining the point at which maximum greenhouse warming occurs the g = 30 ms^{-2}, but they do not strongly affect the surface temperature for a given CO_2 column amount at lower pressures. The atmosphere begins to collapse before the surface temperature reaches the water melting point only in the most conservative g = 30 ms^{-2} case. [32]

2. Re-entry rockets into the atmosphere

A rocket re-entering the earth's atmosphere experiences a drag force proportional to the square of its speed and proportional to air density. This ρ density is approximately given by the law: $\rho = \rho_0 e^{-\lambda z}$, where z is the height above the earth; ρ_0 is the density at sea level, and λ is a positive constant.

Be A area of rocket straight section; C_D called a constant drag coefficient, and we assume that the re-entry is vertical, and without support. The second law of Newtonm the equation of motion is:

$$mv\frac{dv}{dz} = -mg + \frac{1}{2}C_D A \rho v^2 \qquad (1)$$

Note that we are measuring the acceleration up. It is more convenient as well. Imagine you throw a stone up and then just consider his fall to the ground. In this example, the rocket should slow down when approaching the Earth and thus the resulting force must be up

As:

$$\frac{dv}{dz}(v^2) = 2v\frac{dv}{dz}$$

therefore wrote $V = v^2$ and $K = C_D A/m$, then we get:

$$\frac{dv}{dz}(v^2) = -2g + \frac{C_D A}{m}\rho v^2$$

i.e.:

$$\frac{dv}{dZ} = -2g + K\rho_0 e^{-\lambda z} V$$

or:

$$\frac{dv}{dZ} - K\rho_0 e^{-\lambda z} V = -2g$$

The integration factor is:

$$e^{\int -K\rho_0 e^{-\lambda z} dz} = e^{(K/\lambda)\rho_0 e^{-\lambda z}}$$

multiplying the equation of motion for this fact:

$$\frac{d}{dz}(Ve^{(K\rho_0/\lambda)e^{-\lambda z}}) = -2ge^{(K/\lambda)\rho_0 e^{-\lambda z}}$$

that integrating gives:

$$Ve^{(K\rho_0/\lambda)e^{-\lambda z}} = \int -2ge^{(K/\lambda)\rho_0 e^{-\lambda z}} dz$$

if we expand $e^{(K\rho_0/\lambda)e^{-\lambda z}}$ in a Maclaurin series and integrating term by term, we obtain:

$$V = e^{(-K\rho_o/\lambda)e^{-\lambda z}}\left[-\frac{2g}{\lambda}\sum_{n=1}^{\infty}\frac{\left(\frac{\rho_0 K}{\lambda}e^{-\lambda z}\right)^n}{n \cdot n!} - 2gz + constant\right] \tag{2}$$

This equation is very laborious to obtain a *V* calculated at various points of the rocket descent. It is not feasible to use it for a qualitative information. [34, 35]

2.1 Runge-Kutta Method
The method of the fourth order Runge-Kutta method to a rocket reentry problem in the atmosphere, requires four evaluations for the function *f(x,y)*, in case the speed with altitude z, is the particular combination of this gives us an estimate equivalent y to the Taylor expansion up the term $(x - x_0)^4$.

Two sizes steps were used. The dashed line indicates the numerical solution, "badly behaved", with increased rocket speed, because it was not used in this no instruction to predict this. It can be seen that the Runge-Kutta method is almost independent of the two sizes rungs.

In order to verify the effects of gravity, the calculations were repeated without this. An outline of it is given by the Fig. (3-left) . The Runge-Kutta method is the most accurate of the three methods, Euler, Euler perfected and Runge-Kutta for the two steps with and without gravity *g*.

3. Atmospheric entry

As a space vehicle approaches a planet having an atmosphere, it experiences an approximate exponentially increasing atmospheric density. This provides a changing aerodynamic

environment for the vehicle. Initially the Mach number (the ratio of the vehicle's speed relative to the local speed of sound in the gas) *Mo* may be in the range of 20 to 50. The initial density is so low, however, that the flow field is described as a *free molecular flow*. In this regime, the molecules and atoms that constitute the atmosphere collide so infrequently, that following impact upon a vehicle surface, the molecule will not then collide with the incoming molecules. Under such conditions, shock waves are not formed about the body. However, as the vehicle progresses further into the atmosphere, a transition *flow* commences. This region is difficult to describe analytically, and frequently *bridging functions* are used to describe the aerodynamic properties of the vehicle. Thick viscous shock waves are formed about the vehicle at this time. Eventually, if the vehicle penetrates sufficiently low in the atmosphere, a *continuum flow* region is encountered, which is that type of flow typified by conventional aerodynamics. The velocity, however, is still so great that the flow remains hypersonic. [36]

Key to an understanding of the flow field and the changes that occur within it is the recognition of the amount of energy required to be dissipated. Taking the amount of energy per unit mass to be $\sim 0.5V^2$, if a vehicle is approaching the planet on a hyperbolic trajectory with a velocity of tens of km/s, hundreds of MJ must be dissipated. An extreme example is the entry of the Galileo probe into the Jovian atmosphere in 1995. With an approach speed of $47.5 km/s$, $3.8 \times 10^5 MJ$ of translational energy were dissipated in the four minutes before the drogue parachute was deployed. This generated a temperature of 15000K, and an estimated 90kg of ablative material was lost from the probes forward heat sltield (out of a total probe initial mass of 340 kg). At such energies, the gas that is incident upon the vehicle undergoes not only chemical reactions, but also excitation of internal energy modes such as vibration, together with dissociation and ionization. Relaxation from these excited states may arise through radiation. The time constants of these processes are large, and hence the flow field is not in equilibrium. As a result, there is great difficulty in analytically predicting the changes that arise in the gas, as the normal relationships of equilibrium thermodynamics cannot be applied. Approximations, such as assuming that the constituents (both in terms of their chemical composition and the degree to which excitation has occurred) have relative number density fractions frozen at some point in the flow, may be used to simplify the analysis. Detailed predictions are made yet more complex by the uncertain role the vehicle surface plays in the chemistry of the reacting flow. The overall net effect however, of the high velocity flow field impinging on a surface is to cause substantial heat transfer to the vehicle. It is also clear from this brief introduction that, because of the chemically reacting flow conditions, the actual heat loads a vehicle will experience will depend upon the constituents of the atmosphere itself. [36]

4. Constraints during atmospheric entry

The two principal constraints that occur in the design of an aeromanoeuvring vehicle are the peak dynamic load and the peak thermal load, together with how long these loads exist.

During entry, it is possible to write down the overall governing equations that describe the dynamics. For a ballistic entry, it is assumed that the aerodynamic forces only provide a drag force parallel to the instantaneous direction of motion, with no cross track force (equivalent to a zero for the lift coefficient C_L) It is possible to write down the relationship between the distance to the centre of the planet r at time t, if at that time the flight angle of the vehicle is γ and the velocity V. Assuming the density at some reference height his given by ρ_s which decreases exponentially with a scale height of β, then following, [36, 37]

$$\frac{dr}{dt} = V \sin\gamma \tag{3}$$

where

$$\frac{dV}{dt} = -\frac{1}{2}\rho_s V^2 e^{-\beta h}\frac{SC_D}{m} = -\eta\beta V^2 \tag{4}$$

Here a dimensionless height variable η has been introduced,

$$\eta = \frac{1}{2}\rho_s\frac{SC_D}{m}\frac{1}{\beta}e^{-\beta h} \tag{5}$$

The ballistic coefficient, $\frac{SC_D}{m}$, where S is the wened surface area for a vehicle of mass m having a drag coefficient C_D, is seen from equation (4) to provide a linear influence over the rate at which the vehicle decelerates. However, the maximum deceleration for an initial speed V_0 and entry angle γ_0 is given by δ_{max} and is found to be independent of the ballistic coefficient,

$$\delta_{max} = \frac{\beta V_0^2}{2e}\sin\gamma_0 \tag{6}$$

Turning to the peak-heating load, it is clear from the discussion above that a simple analytic description is not available, if one wishes to describe the real flow situation. Approximations may be used to provide some estimate of the heating profile. These typically omit elements of the various heat transfer processes that take place in the real flow. For example, if only convective heat transfer is considered (or is indeed dominant), [37] then the peak heating rate is given by

$$\dot{q}_{max} \propto V_0^3\sqrt{\frac{m\beta\sin\gamma_0}{3SC_D}} \tag{7}$$

In general, this peak heat flux will occur at a different altitude from that for the peak deceleration load. Evidently, both the dynamics and heat loads are dependent upon the initial conditions assumed for atmospheric entry. [38] As a result, calculations that are performed must assume an overall mission profile. Thus, the preceding interplanetary manoeuvres will influence the final loads experienced by a vehicle, together with the launch date. Thus, for the Mars Pathfinder mission, [39] the inertial arrival velocity could vary by l00 m/s. [36]

5. Discussions

It was found that above 30,000 m, the discrepancy is less than 0.5%, but quickly increases, decreasing in altitude. Already shown in Fig. (3), that the exclusion of gravity is less important for higher speeds of reentry. If we return to the analytical solution, then the omission of gravity produces (see equation (2)):

$$V = constant \times e^{(-K\rho_o/\lambda)e^{-\lambda z}} \tag{8}$$

so that:

$$v = constant \times e^{(-K\rho_o/2\lambda)e^{-\lambda z}} \tag{9}$$

(constant factor, $v = \sqrt{V}$)

The altitude of the order of 100 km, the exponential term $\cong 1$ if mg/C_DA is large enough, if v_e is the re-entry speed at that speed:

$$v = v_e \times e^{(-K\rho_o/2\lambda)e^{-\lambda z}} \tag{10}$$

This is one of a chain approximations but illustrates the use of a simple method based on more complicated physical situations. thus showing how reliable are the estimates of Runge-Kutta, Fig. (3). [34, 35]

The ballistic coefficient, $\frac{SC_D}{m}$, where S is the wened surface area for a vehicle of mass m having a drag coefficient C_D, is seen from equation (4) to provide a linear influence over the rate at which the vehicle decelerates. However, the maximum deceleration for an initial speed V_0 and entry angle γ_0 is given by δ_{max} and is found to be independent of the ballistic coefficient, equation (6)

$$\delta_{max} = \frac{\beta V_0^2}{2e}\sin\gamma_0$$

In general, this peak heat flux will occur at a different altitude from that for the peak deceleration load. Evidently, both the dynamics and heat loads are dependent upon the initial conditions assumed for atmospheric entry. [38] As a result, calculations that are performed must assume an overall
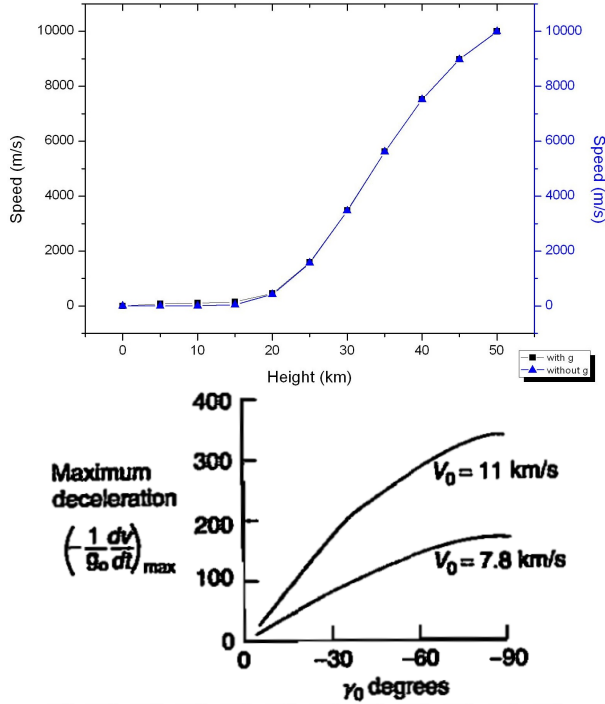
Figure 2. Graphic (Up) of speed(v) in m/s with altitude, height(z) in km, see equation (2) for Runge-Kutta Method [35]. Ballistic entry characteristics from variation of the maximum deceleration with entry angle γ_o and entry speed V_o for ballistic entry (Down), see equation (6). [35, 40]

mission profile and the inertial arrival velocity could vary by l00 m/s. [36]

Returning to equation (2) to a practical application having the data values:

$k = C_D A/m, C_D = 1; A = 1; m = 1000$, then

$k = 1 \times 1/1000 = 10^{-3}$.

$\lambda = 1; \rho_o = 1000 = 10^3; g = 10$ and $n = 1, 2, 3$, all in S.I.

Analysing φ as the term in equation (2):

$$\varphi = e^{(-K\rho_o/\lambda)e^{-\lambda z}} \tag{11}$$

from $z \Rightarrow$ very large value, this means that $\varphi = 1$, then equation (2) is as:

$$V = \left[-\frac{2g}{\lambda} \sum_{n=1}^{\infty} \frac{\left(\frac{\rho_0 K}{\lambda} e^{-\lambda z} \right)^n}{n \cdot n!} - 2gz + constant \right] \tag{12}$$

$$V = -20 \left[e^{-z} + e^{-2z} + e^{-3z} - z + constant \right] \tag{13}$$

like $V = v^2$

$$v^2 = 20z + constant \Rightarrow v = \sqrt{20z + constant} \tag{14}$$

which is the *Torricelli equation* [41, 42] for $g = 10$.

6. Conclusions

Being that GJ581d was the first planet candidate of a few Earth masses reported in the circum-stellar habitable zone of another star. It is located a star, a red dwarf about 20 light years away from Earth. [2] It has been suggested that the GJ581d might be able to support liquid water due to its relatively low mass and orbital distance. Its mass is thought to be 6.98 Earths$(\oplus)$ and its radius is thought to be $2.2R_\oplus$. Given this relation and the current uncertainties in Gl 581d's mass, we can expect the planet's surface gravity to be in the range $10 - 30ms^{-2}$. According to the model is originally based on the one described by Kasting et al [22, 23, 24, 25] Mischna et al. [26] and Pavlov et al. [27]

Under such conditions, it is unknown whether any habitable climate on the planet would be able to withstand global glaciation and / or atmospheric collapse.

This model considers N_2, H_2O, and CO_2 as atmospheric gases. The presence of these gases highly depends on the planetary scenario (e.g., outgassing, volcanism, formation, biosphere), our model atmospheres are restricted to the two most important greenhouse gases of the Earth's atmosphere (H_2O and CO_2), using N_2 as additional backgroundgas. The climate that demonstrate GJ581d will have a stable atmosphere and surface liquid water for a wide range of plausible cases, making it the first confirmed super-Earth in the habitable zone.

According to the general principle of relativity:

"All systems of reference are equivalent with respect to the formulation of the fundamental laws of physics." [43, 44]

In this case all the equations studied apply to the exoplanet Gliese 581d.

If humanity is able to send a probe to Gliese 581d, this has all the mathematical conditions set it down successfully on its surface.

References

[1] J. E. Gizis S. L. Hawley and N. I. Reid. The palomar/msu nearby star spectroscopic survey.ii.the southern m dwarfs and investigation of magnetic activity. *Astronomical Journal*, 113:1458, April 1997. doi: 10.1086/118363.

[2] National Geographic Channel. Exoplaneta aurélia. NGC, March 2010.

[3] S. Udry; X. Bonfilis; X. Delfosse et al. *Astron. Astrophys.*, 469(L43), 2007.

[4] M. Mayor et al. The harps search for southern extra-solar planets. xviii. an earth-mass planet in the gj 581 planetary system. *Astron. Astrophys.*, 507:487–494, 2009.

[5] E. J. Rivera N. Haghighipour G. W. Henry S. S. Vogt, R. P. Butler and M. H. Williamson. The lick-carnegie exoplanet survey: A 3.1 mearth planet in the habitable zone of the nearby m3v star gliese 581. *The Astrophysical Journal*, (723):954–965, 2010.

[6] PHL's Exoplanets Catalog Planetary Habitability Laboratory, April 2016.

[7] J. F. Kasting; D. P. Whitmire and R. T. Reynolds. *Icarus*, 101(108), 1993.

[8] R. T. Pierrehumbert. A palette of climates for gliese 581g. *The Astrophysical Journal Letters*, (726):L8+, January 2011. doi: 10.1088/2041-8205/726/1/L8.

[9] R. A. Kerr. First goldilocks exoplanet may not exist. *Science*, 330(6003):433, 2010. doi: 10.1126/science.330.6003.433.

[10] M. Tuomi. Bayesian re-analysis of the radial velocities of gliese 581. evidence in favour of only four planetary companions. *Astronomy and Astrophysics*, (528):L5+, April 2011. doi:10.1051/0004-6361/201015995.

[11] R. D. Wordsworth; F. Forget; F. Selsis; E. Millour; B. Charnay and J. B. Madeleine. Gliese 581d is the first discovered terrestrial-mass exoplanet in the habitable zone. *Cornell University Library*, 2011. arXiv:1105.1031v1.

[12] R. D. Wordsworth; F. Forget; F. Selsis; E. Millour; B. Charnay and J. B. Madeleine. Gliese 581d is the first discovered terrestrial-mass exoplanet in the habitable zone. *The Astrophysical Journal Letters*, (733):L48 (5pp), June 1 2011. doi:10.1088/2041-8205/733/2/L48.

[13] W. von Bloh et al. "the habitability of super-earths in gliese 581". *Astronomy and Astrophysics (Astronomy & Astrophysics)*, 3(1365-71):476, 2007. arXiv:0705.3758. Bibcode:2007A&A...476.1365V. doi:10.1051/0004-6361:20077939.

[14] W. von Bloh et al. Habitability of super-earths: Gliese 581c & 581d. *Proceedings of the International Astronomical Union (International Astronomical Union)*, 3(S249):503–506, 2008. arXiv:0712.3219. doi:10.1017/S1743921308017031.

[15] R. Wordsworth; F. Forget; F. Selsis; J.-B. Madeleine; E. Millour and V. Eymet. Is gliese 581d habitable? some constraints from radiative-convective climate modeling. *Astronomy and Astrophysics*, (522):A22+, 2010b. doi: 10.1051/0004-6361/201015053.

[16] P. von Paris; S. Gebauer; M. Godolt; J. L.. Grenfell; P. Hedelt; D. Kitzmann; A. B. C. Patzer; H. Rauer and B. Stracke. The extrasolar planet gliese 581d: a potentially habitable planet? *Astronomy and Astrophysics*, (522):A23+, November 2010. doi: 10.1051/0004-6361/201015329.

[17] L. Kaltenegger; A. S. Peralta; and S. Mohanty. Model spectra of the first potentially habitable super-earth - gl581d. *Accepted for publication in The Astrophysical Journal*, March 2011.

[18] F. Pepe et al. *Astron. Astrophys.*, 534:A58, 2011.

[19] G. Anglada-Escudé and M. Tuom. Comment on "stellar activity masquerading as planets in the habitable zone of the m dwarf gliese 581". *Science*, 347(6226):pp 1080, 6 Mar 2015. doi:10.1126/science.1260796.

[20] S. Seager; M. Kuchner; C. A. Hier-Majumder and B. Militzer. "mass-radius relationships for solid exoplanets". *The Astrophysical Journal*, (669):1279–1297, 2007. DOI:10.1086/521346. Retrieved on 2015-11-14.

[21] Gliese 581 d. Wikimedia Commons, the free media repository, October 4 2010. Creative Commons. (CC BY-SA 3.0).

[22] J. F. Kasting; J. B. Pollack and T. P. Ackerman. *Icarus*, (57):335, 1984a.

[23] J. F. Kasting; J. B. Pollack and D. Crisp. *J. Atmospheric Chem.*, (1):403, 1984b.

[24] J. F.Kasting. *Icarus*, (74):472, 1988.

[25] J. F.Kasting. *Icarus*, (94):1, 1991.

[26] M. A. Mischna; J. F. Kasting; A. Pavlov and R. Freedman. *Icarus*, (145):546, 2000.

[27] M. A. Mischna; J. F. Kasting; A. Pavlov and R. Freedman. *Icarus*, (145):546, 2000.

[28] P. von Paris; H. Rauer; J. L. Grenfell et al. *Planet. Space Science*, (56):1244, 2008.

[29] S. Manabe and R. T. Wetherald. *J. Atmosph. Sciences*, (24):241, 1967.

[30] F. Montmessin; B. Gondet; J. Bibring et al. *JGR (Planets)*, 112(11), 2007.

[31] F. Forget and R. T. Pierrehumbert. *Science*, 278(1273), 1997.

[32] R. D. Wordsworth; F. Forget; F. Selsis; J. B. Madeleine; E. Millour and V. Eymet. Is gliese 581d habitable? some constraints from radiative-convective climate modeling. *Astronomy & Astrophysics. ESO 2010. arXiv:1005.5098v2 [astro-ph.EP]*, (15053 b), October 18 2010.

[33] C. Sotin; O. Grasset and A. Mocquet. *Icarus*, 191(337), 2007.

[34] A. C. Bajpai and L. R. Mustoe. *Engineering Mathematics*. John Wiley & Sons Ltd., 1979.

[35] A. C. Bajpai; L. R. Mustoe and D. Walker. *Matemática para Engenharia*. Hemus, 1980.

[36] P. Fortescue; J. Stark and G. Swinerd. *Spacecraft Systems Engineering*. John Wiley & Sons Ltda., third edition edition, 2003.

[37] N. X. Vinh; A. Busemann and R.D. Culp. *Hypersonic and Planetary Entry Flight Mechanics*. University of Michigan Press, Michigan, 1980.

[38] L. Lees; F. W. Hastwig and C.B. Cohen. Use of aerodynamic lift during entry into the earth's atmosphere. *Am. Rocket Soc. J.*, pages 633–641, September 1959.

[39] D. A. Spenser and R. D. Braun. Mars pathfinder atmospheric entry: trajectory design and dispersion analysis. *J. Spacecraft Rockets*, (33):670–676, 1996.

[40] N. X. Vinh; A. Busemann and R. D. Culp. *Hypersonic and Planetary Entry Flight Mechanics*. University of Michigan Press, Michigan, 1980.

[41] R. Resnick; D. Halliday and K. S. Krane. *Physics*, volume 1-4. Livros Técnicos e Científico S.A. (LTC), 5 edition.

[42] P. A. Tippler. *Física*, volume 1-2. LTC, 2002.

[43] C. Møller. *The Theory of Relativity*. Delhi: Oxford University Press, 2nd ed. edition, 1952. ISBN 0-19-560539-X.

[44] Ø. Grøn and S. Hervik. *Einstein's General Theory of Relativity*. Oslo, Norway; Cambridge, United Kingdom.

[45] Sunset of the habitable worlds. PHL UPR Arecibo, July 2 2012.

[46] K. Wehrstein. Astronomy picture of the day. Sunrise from the surface of gliese 581c. NASA, May 2 2207.

7. Attachments

This Figure (3) shows an actual image of a sunset on Earth compared to artistic representations for the best candidates of potential habitable worlds so far. The image corrects for the size, colors, and brightness of the star and sky as seen from an Earth-like world located in the orbits of these worlds. The size of and colors of the star of Kepler-22 b look similar to Earth because it orbits a Sun-like star. The sunsets of Gliese 667Cc and 581d look much redder because they orbit a red dwarf star, with the sky of Gliese 581d much darker due to its greater distance. The star of HD 85512b is the brightest of all cases although the star of Gliese 667Cc is the biggest. [45]

How might a sunrise appear on Gliese 581c? One artistic guess is shown Figure (4). Gliese 581c is the most Earth-like planet yet discovered and lies a mere 20 light-years distant. The central red dwarf is small and redder than our Sun but one of the orbiting planets has recently been discovered to be in the habitable zone where liquid water could exist on its surface. Although this planet is much different from Earth, orbiting much closer than Mercury and containing five times the mass of Earth, it is now a candidate to hold not only oceans but life enabled by the oceans. Were future observations to confirm liquid water, Gliese 581c might become a worthy
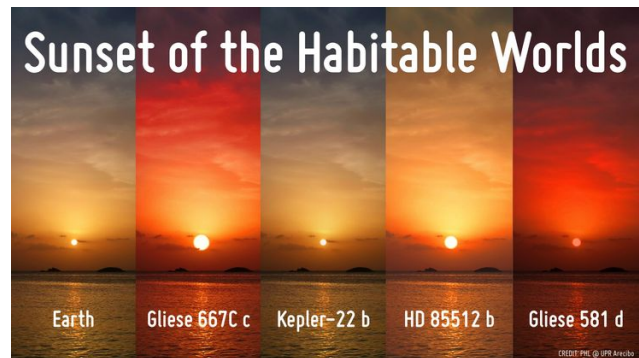

Figure 3. This figure shows an actual image of a sunset on Earth compared to artistic representations for the best candidates of potential habitable worlds so far. [45]
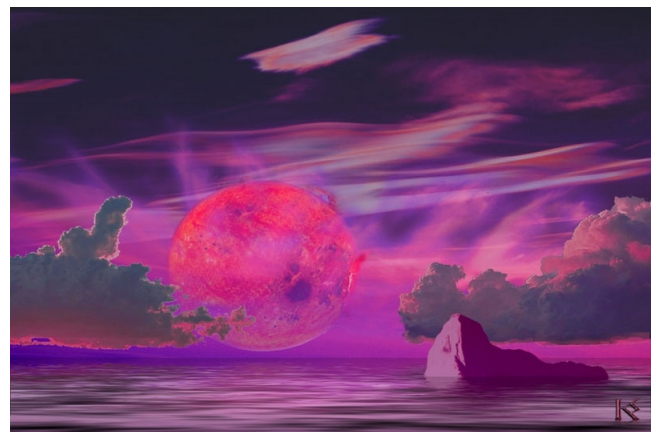
Figure 4. This figure shows an sunrise from the Surface of Gliese 581c. [46]

destination or way station for future interstellar travelers from Earth. Drawn above in the hypothetical, the red dwarf star Gliese 581 rises through clouds above a calm ocean of its planet Gliese 581c. [46]